

Test and characterization of a prototype silicon-tungsten electromagnetic calorimeter

Sanjib Muhuri^a, Sourav Mukhopadhyay^b, Vinay B. Chandratre^b, Menka Sukhwani^b, Satyajit Jena^c, Shuaib Ahmad Khan^a, Tapan K. Nayak^a, Jogender Saini^a, Rama Narayana Singaraju^a

^aVariable Energy Cyclotron Centre, Kolkata - 700064, India

^bBhabha Atomic Research Centre, Electronics Division, Trombay, Mumbai - 400085, India

^cIndian Institute of Technology, Bombay, Mumbai - 400076, India

Abstract

New generation high-energy physics experiments demand high precision tracking and accurate measurements of a large number of particles produced in the collisions of elementary particles and heavy-ions. Silicon-tungsten (Si-W) calorimeters provide the most viable technological option to meet the requirements of particle detection in high multiplicity environments. We report a novel Si-W calorimeter design, which is optimized for γ/π^0 discrimination up to high momenta. In order to test the feasibility of the calorimeter, a prototype mini-tower was constructed using silicon pad detector arrays and tungsten layers. The performance of the mini-tower was tested using pion and electron beams at the CERN Proton Synchrotron (PS). The experimental results are compared with the results from a detailed GEANT-4 simulation. A linear relationship between the observed energy deposition and simulated response of the mini-tower has been obtained, in line with our expectations.

Keywords: Calorimeter, electromagnetic shower, silicon pad detectors

1. Introduction

One of the major challenges in high-energy physics experiments is to detect and analyze majority of the particles produced in the collisions of elementary particles or heavy-ions. Experiments at the CERN Large Hadron Collider (LHC) and at the planned colliders (International Linear Collider or Future Circular Collider) necessitate accurate energy measurements over a large dynamic range and high precision tracking of the particles emitted in the collisions. Compared to proton-proton collisions, the challenges get manifold for the heavy-ion (such as Pb-Pb) collisions due to the increase in the number of emitted particles by several orders of magnitude. A calorimeter [1] is normally used for accurate characterization of an incoming particle in terms of its position and energy. Sampling calorimeters, segmented in longitudinal as well as in transverse directions, are considered to be ideal for accurate characterization of particles in terms of their positions and energies.

In this article, we consider Si-W calorimetry, using tungsten as converters/absorbers and segmented silicon pad detectors as active medium. Because of good energy and position resolution characteristics, silicon de-

tectors are considered to provide the most suitable detection medium. Although the silicon pad detectors used here have no intrinsic charge gain, they exhibit good charge collection efficiency, fast response time and require low bias voltage to achieve full depletion. Low sensitivity of silicon detectors to the magnetic field enables the calorimeter to be compatible with complex experimental setup in high magnetic field environment. At the same time, use of tungsten as absorber makes the electromagnetic calorimeter relatively compact and helps to achieve full energy containment. Combination of silicon and tungsten layers offer one of the most novel design for calorimetry in high energy physics experiments [2, 3, 4, 5, 6, 7, 8, 9, 10, 11, 12, 13, 14, 15].

In this article we report the design of a Si-W calorimeter, which can provide accurate position and energy measurement with minimum leakage in both transverse and longitudinal directions. In order to test the feasibility of such a design, a mini-tower, consisting of four layers of silicon pad detectors and tungsten plates as absorbers, has been constructed. The design, performance and characterization of the mini-tower has been discussed in detail. Though the prototype is limited with a few course layers, the basic characteristics,

like, longitudinal shower profile, calibration of energy deposition, etc., can aid to build the full length calorimeter. The article is organized as follows. Section 2 gives the design of the Si-W calorimeter and in section 3, setup of the mini-tower is discussed. Details of the silicon pad detector arrays with readout electronics are discussed in section 4. In section 5, the laboratory test results of silicon pad detector with β -source is presented. The test beam setup is given in section 6. The results of the energy deposition from simulated and experimental data have been described and compared in section 7. The article is concluded with a summary in section 8.

2. Design of a Si-W Calorimeter

A sampling type electromagnetic calorimeter with silicon detector as active medium and high purity tungsten as absorber has been simulated using GEANT4 toolkit [16, 17]. The main goal is to optimize the design with adequate energy and position resolutions in order to handle extreme high particle density environment. The design consisted of 20 layers of silicon pad arrays and tungsten combinations. Each layer consisted of a 3.5 mm thick tungsten plate followed by a 0.3 mm thick silicon sensor. In the simulation, pure tungsten with density of 19.3 gm/cm^3 has been used. Being a high-Z element, tungsten converts high energy photons or electrons into electromagnetic showers. The majority of the photons that are emitted in high energy collisions are decay photons from π^0 mesons. One of the major goals is to reconstruct π^0 mesons and their energy from the measured photon showers. The decay angle of the two emitted photons decreases with the increase of the energy of π^0 mesons. The reconstruction of the photon showers needs to be accurate in order to obtain the shower positions of the photons and deposited energy. In order to measure π^0 energy accurately, tracking of the shower in different layers is needed. Therefore, the good position resolution of the detectors in the sensitive medium is essential.

The calorimeter, shown in Figure 1, was designed considering all of the above requirements into account [14]. Three high granular planes were placed in the region of the shower maxima for accurate measurements. Twenty sensitive detector layers were considered, out of which three layers (4, 8 and 12) were made of highly granular silicon pads, each with dimension of $0.1 \text{ cm} \times 0.1 \text{ cm}$. The rest of the layers were made up of $1 \text{ cm} \times 1 \text{ cm}$ silicon pad detectors. The three high granular planes help to determine the shower position with high accuracy and thus help in tracking the path of the incoming particles. Reconstruction of clusters

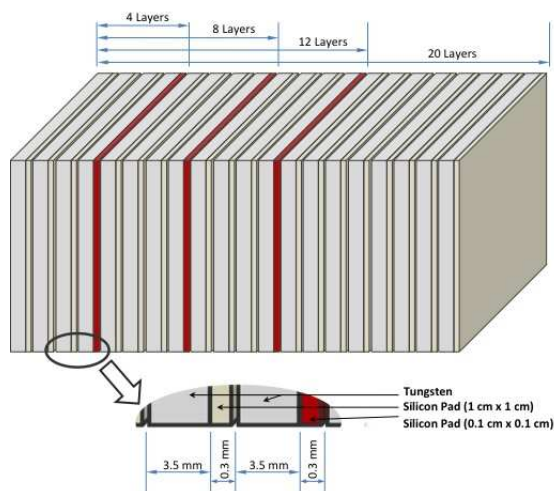


Figure 1: The components of a tungsten-silicon sampling calorimeter consisting of 20 layers of detectors. The three highlighted layers are made of highly granular $0.1 \text{ cm} \times 0.1 \text{ cm}$ silicon pads, and the rest of the layers consist of $1 \text{ cm} \times 1 \text{ cm}$ silicon pads.

(produced from electromagnetic showers of electrons or photons at consecutive layers) using the Fuzzy Clustering technique was carried out and found to be quite powerful in differentiating overlapping clusters [14]. Responses of single particle events (electrons, photons, π^\pm and π^0) were obtained by placing the calorimeter at a distance of 400 cm from the interaction point. The performance of the calorimeter has been found to be efficient in discriminating γ to π^0 up to 200 GeV. The feasibility of the calorimeter has further been studied by constructing a mini-tower and testing it with pion and electron beams of various energies.

3. Mini-tower arrangement

The prototype tests of the Si-W calorimeter were performed with the help of two different setups of the mini-tower by using four layers of silicon pad detector arrays with readout electronics and several tungsten plates. Each of the tungsten plates is 1 radiation length (X_0) thick and with 99.9% purity. The setups are considered by keeping in mind the more realistic case to be implemented in future experiments. Both the setups are shown in Fig. 2. In Setup-1, four layers of tungsten and silicon pad detector arrays are placed alternatively. This gives the response of incoming particles up to $4 X_0$ in longitudinal depth. In Setup-2, two additional tungsten layers are placed in front to extend the depth up to $6X_0$.

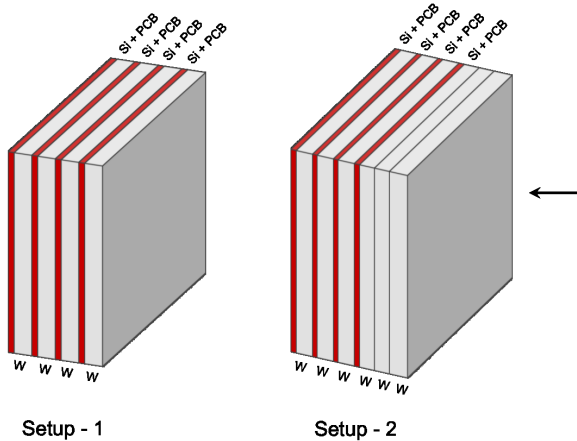


Figure 2: Two different setups of the mini-tower arrangement used for the test at CERN-PS.

4. Silicon pad array and associated electronics

Each plane of the mini-tower consists of an array of 5×5 single element silicon pads as shown in Fig. 3. Each silicon pad is of $1 \text{ cm} \times 1 \text{ cm}$ size and $300 \mu\text{m}$ thick. The silicon detectors are fabricated on $\langle 111 \rangle$ FZ n-type wafers with $3 - 5 \text{K-}\Omega\text{-cm}$ resistivity. The top pads are p+ and the bottom side is n+. The leakage current of the detectors is less than a few nA and breakdown voltage is above 250 V. Each of the detectors is surrounded by a guard-ring and is appropriately biased. The silicon pads have full depletion capacitance of 40 pF/cm^2 at 60 V. Silicon pads are mounted on a 0.8 mm thick four layer PCB, both to hold and to connect to readout electronics. The detectors were attached to the PCB with silver conductive epoxy of resistivity $0.006 \Omega\text{-cm}$. The top of the diode was coated with $1 \mu\text{m}$ thick Al and $0.5 \mu\text{m}$ thick phosphosilicate glass (PSG) passivation. Possibility of cross talk among the silicon pad elements is negligible because the detectors are physically isolated from each other.

The detector signals were readout using Front End Electronics (FEE) boards. Two different kinds of ASICs, namely, MANAS [18, 19] and ANUSANSKAR were used. Both ANUSANSKAR and MANAS ASICs incorporate 16 pulse processing channels along with analog multiplexed output. Each channel is comprised of a Charge Sensitive Amplifier (CSA), second order semi Gaussian pulse shapers, track and hold (T&H) circuit and output buffer. For ANUSANSKAR, AMI Semiconductor $0.7 \mu\text{m}$ C07-MA technology has been used whereas for MANAS, SCL $1.2 \mu\text{m}$ C1D twin tub process have been adopted. The size of the input transistor for both the ASICs is $8000 \mu\text{m}/1.5 \mu\text{m}$. In ANUSAN-

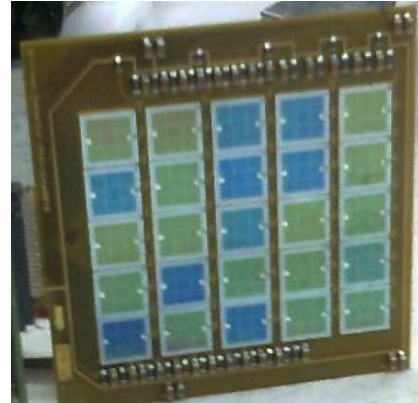


Figure 3: (Color online) Sketch of the silicon detector array consisting of 5×5 single element silicon pad detectors.

SKAR, CSA design is based on conventional folded cascode architecture with high value of feedback resistor, which is implemented through current conveyor method with improved linearity for large signals. As the input transistor plays a vital role in determining the noise performance of the whole amplifier, large area p-type MOS transistor is used as the input device to reduce the flicker noise. The input transistor is biased in sub threshold region with $500 \mu\text{A}$ bias current, ensures appropriate transconductance (g_m) to reduce the contribution due to thermal noise. Semi-Gaussian shaping is implemented using 2nd order Sallen-key filter with wide swing Operational Transconductance Amplifier (OTA) and with a peaking time of $1.2 \mu\text{s}$. However, semi Gaussian shapers inside MANAS are implemented through Gm-C filter topology. The baseline recovery better than 1% after $4 \mu\text{s}$ in ANUSANSKAR can be achieved by tailoring the pole-zero locations by external DC voltage control. The T&H block is used to sample the peak information of the shaped signal. All the 16 channel outputs of both the ASICs can be readout serially via analog multiplexer with a clock rate of 1 MHz. Performance summary of both the ASICs are given in Table 1.

5. Tests of silicon pad detector with β -source

Each layer of silicon detector array was tested in the laboratory with ^{90}Sr β -source (with end point energy of 0.546 MeV). The test setup is shown in Fig. 4. The optimum operating voltage of the detector has been determined after performing a voltage scan. It has been observed that the detector can be operated at 60 Volts with reasonably good signal to noise ratio and achieved full depletion. The source is placed on top of one of the triggering scintillator. A two-fold coincidence logic is

Specification	ANUSANSKAR	MANAS
Noise at 0 pF	390 rms electrons	500 rms electrons
Noise slope	$7e^-/pf$	$11.6e^-/pf$
Linear dynamic range	+/- 600 fC	+ 500 fC to -300 fC
Conversion gain	3.3 mV/fC	3.2 mV/fC
Peaking time	1.2 μ s	1.2 μ s
Baseline recovery	1% after 4 μ s	1% after 5 μ s
VDD/VSS	+/- 2.5 V	+/- 2.5 V
Analog readout speed	1 MHz	1 MHz
Power consumption	~15 mW/channel	9 mW/channel
Die area	4.6 mm \times 4.6 mm	4.6 mm \times 2.4 mm
Technology	0.7 μ m standard CMOS	1.2 μ m standard CMOS
Package	CLCC-68	TQFP-48

Table 1: Specifications of the readout ASICS (MANAS and ANUSANSKAR) used in the mini-tower setup and tests.

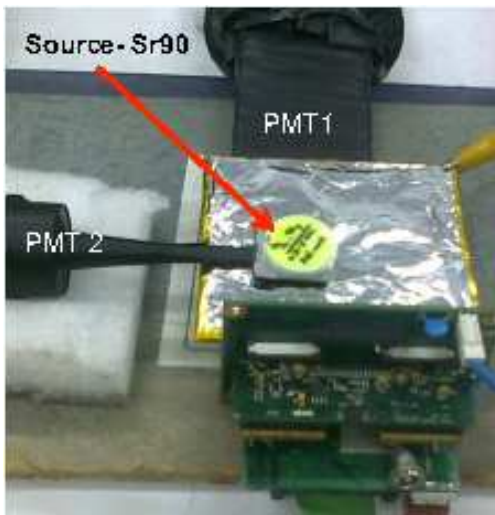


Figure 4: (Color online) Laboratory setup for the test setup of silicon detector array with ^{90}Sr source.

derived using two scintillator paddles as shown in the Fig. 4. Detector response using conventional NIM electronics for each silicon pad element has been carried out extensively. Figure 5 shows typical response for a single silicon pad detector. Part of the noise peak is seen on the left and the signal from the β -source is clearly seen on the right. This elucidates the good functionality of each element of the silicon detector array. To understand the exact detector response and energy loss, tests with pion and electron beams have been performed.

6. Test Beam Setup

Experimental studies with the mini-tower arrangement has been carried out at the T10 beam line of

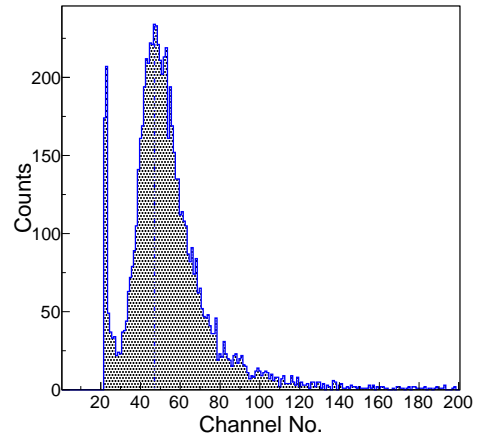


Figure 5: (Color online) Response of a single silicon pad detector to ^{90}Sr source. A clear peak corresponding to β energy of 0.546 MeV is visible on the right, well separated from the noise (see on on the left).

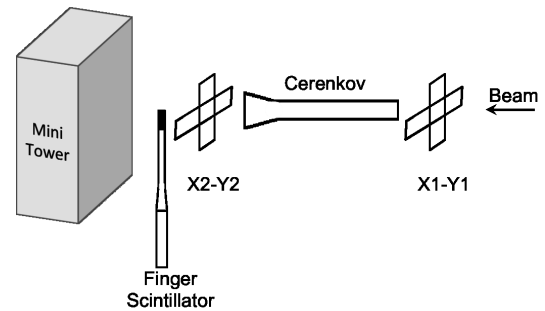


Figure 6: (Color online) Sketch of the detector setup of silicon and tungsten layers.

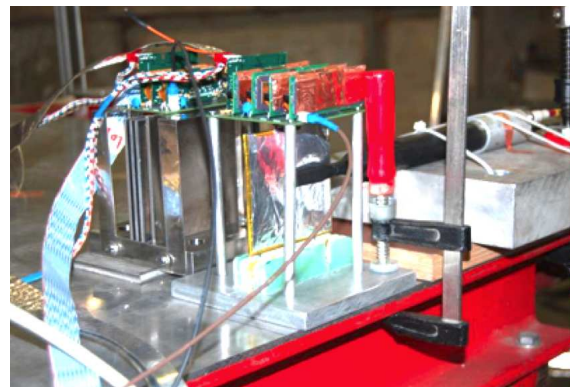


Figure 7: (Color online) Photograph of the experimental Setup used in T10 PS Beam Line facility at CERN

CERN-PS. The T10 beam is a secondary beam that delivers secondary particles up to 7 GeV/c at a production angle of 61.6 milli-radians. The secondary particles predominantly contain negative pions with a mixture of electrons. A dedicated triggering system was used to select either pion or electron beam. The trigger system consists of two pairs of scintillator paddles, a finger scintillator and a Cherenkov detector. The arrangement of the trigger detectors with respect to the mini-tower is shown in Fig 6. The two pairs of paddle scintillators are arranged to determine the $x - y$ positions of the incoming beam within 1 cm^2 area. The pion trigger is generated using the scintillator paddles in coincidence with a small finger scintillator of size $3 \text{ mm} \times 3 \text{ mm}$, placed close to the mini-tower. Additionally, a Cherenkov detector was used for electron trigger. The gas pressure of the Cherenkov detector was adjusted to obtain highest purity of the electrons.

The mini-tower assembly was placed on a movable table to adjust detector position with respect to the beam. A photograph of the detector setup in the T10 beam line is shown in Fig. 7. The silicon pad arrays, along with backplane PCBs are properly shielded against EMI and ambient light for better signal to noise ratio. The detector signals are readout by using a FEE board and further processed by a MARC ASIC, which communicates with the Cluster Read Out Concentrator Unit System (CROCUS) [18, 19]. Finally, the CROCUS interfaces to the data acquisition system via fibre optic cable.

7. Results and discussion

The test beam results for incident pions and electrons with different mini-tower setups are presented here and compared to those from the simulated data. The simulation takes care of each and every aspect of the actual experimental setup. The gap between two tungsten layers is kept as 0.21 cm, out of which 0.03 cm is for the silicon wafer followed by 0.08 cm thick PCB and the rest 0.1 cm is kept for associated electronics. The PCB and electronics parts are included in the simulation. The simulated data gives the energy deposition in each silicon pad for different incoming beams. Responses from each layer of the detector has been extracted by summing up the signals from each layer. Performances of the detector using both the setups of the mini-tower to photons, electrons and neutral pions of different energies were studied extensively using the simulated data.

The mini-tower was exposed to pion and electron beams. Due to lighter mass and electromagnetic nature, electrons produce shower [20] which propagate through

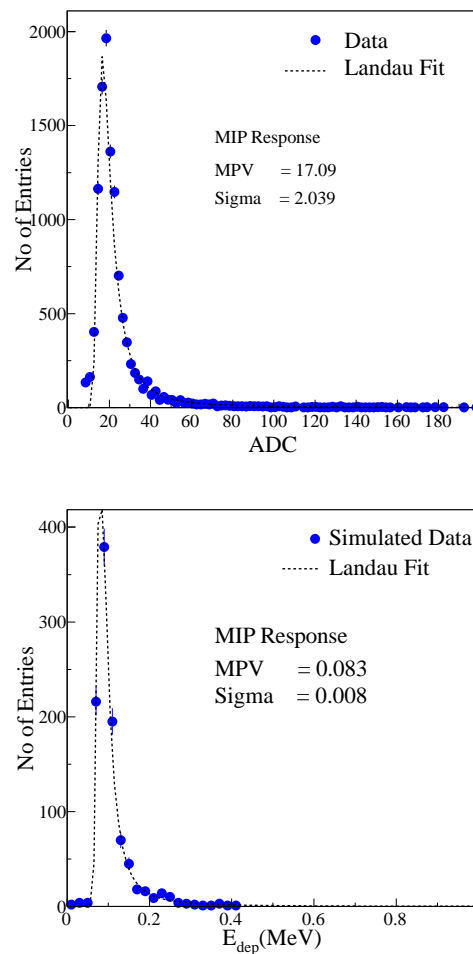


Figure 8: (Color online). Response of silicon pad detector arrays to pions, showing the distribution similar to the minimum ionizing particles: in ADC for test beam data (upper panel) and in MeV from simulated data (lower panel).

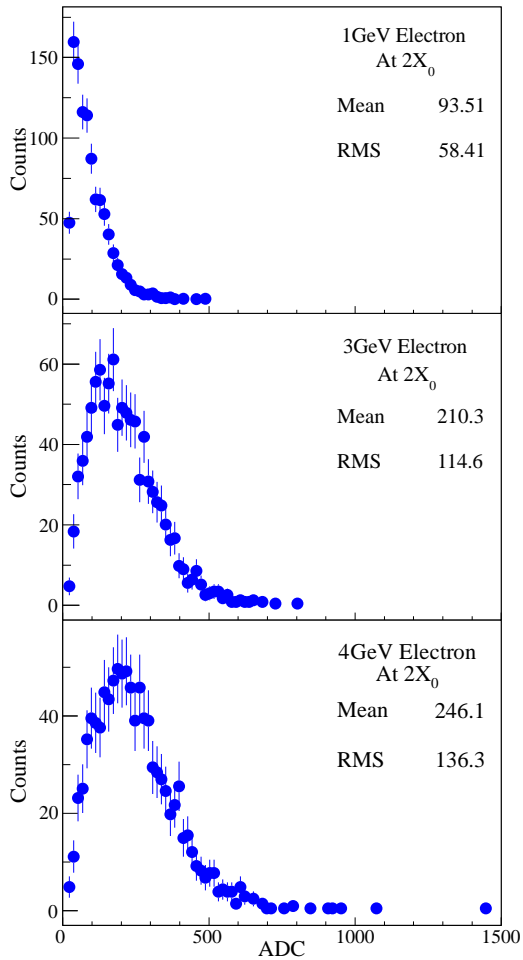


Figure 9: (Color online). Response of silicon pad detector arrays for electrons at three different energies, after $2X_0$ thick tungsten absorber.

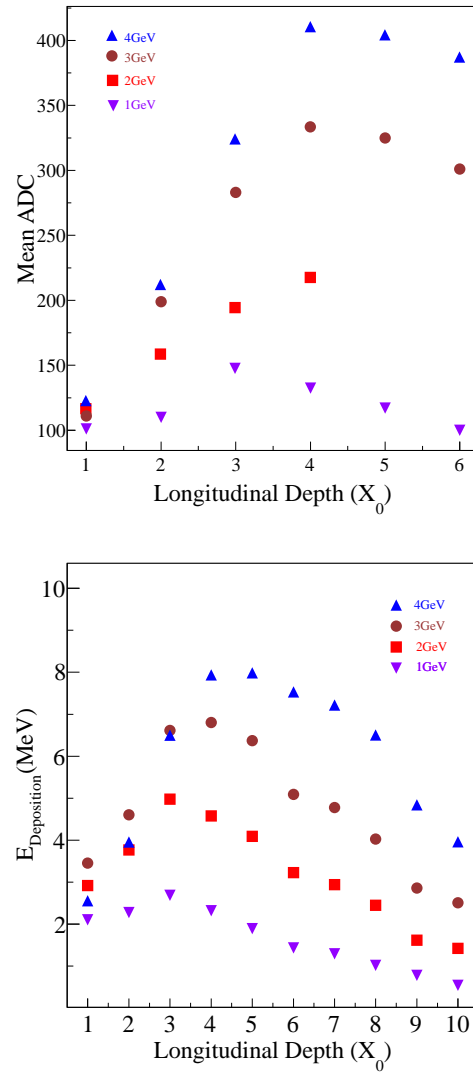


Figure 10: (Color online) Longitudinal shower profile using experimental data (upper panel) and simulated data (lower panel).

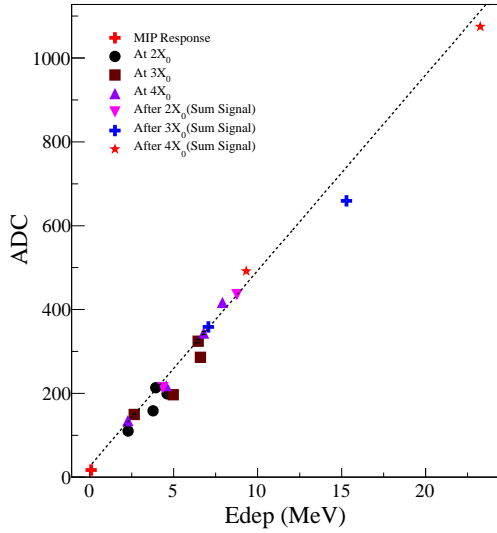


Figure 11: (Color online) Conversion Curve from experimental data (ADC) to energy deposition from simulated data (MeV).

the layers of the tower and leave its footprints for offline reconstruction. Pions are less likely to produce shower within the depth of the calorimeter, and behave like minimum ionizing particles (MIP). The energy deposition of the MIPs can be explained by the Landau Distribution. Analysis of test beam data shows that pions indeed behave like MIP with a most probable value (MPV) of 17 ADC, as shown in the upper panel of Fig. 8. This corresponds to conversion gain of 3.24 mV/fC of the ASIC used. The results of the simulation for pions, shown in the lower panel of Fig. 8 show a similar nature of the MIP spectrum with a MPV value of 83 keV.

Electrons produce electromagnetic shower in the mini-tower. The shower shape and energy deposition in each silicon layer gives an important input for optimizing the granularity along with transverse and longitudinal leakage of energy in the calorimeter. Figure 9 gives the energy deposition of electromagnetic showers produced after $2X_0$ for three different electron energies. It is observed that the shower profile is not so well developed for 1 GeV electron, but as the electron energy increases the distribution becomes more towards Gaussian. The mean of the distributions shift with the increase of energy, as expected.

For different incident energy of electrons, energy depositions are calculated for different silicon pad detector arrays as a function of longitudinal depth from $1X_0$ to $6X_0$. Figure 10 shows the mean energy deposition as a function of longitudinal depth of the mini-tower. The

experimental data, presented in the upper panel, shows that with the increase of the longitudinal depth, the energy deposition for a given incident energy increases at first and then comes to a maximum. Simulated results, as shown in the lower panel of the figure, confirms to the experimental findings. These show that the energy deposition from the resulting shower increases with the increase of depth of the calorimeter until it attains a maximum (shower max) and then deteriorates. The position of the shower max is found to shift to larger depth with increase in the energy of the incident particle. The shower profiles observed in the experimental data are similar to what is expected from the simulation. This is reassuring in the process of making a full calorimeter.

The energy depositions for all combinations of absorber material thickness and beam energies from simulations and the experimental data have been calculated and plotted in Fig. 11. The abscissa gives the energy deposition from simulated data whereas the ordinate shows the experimental observations. For the electron data, signals corresponding to each layer as well as sum of signals from different layers are presented. MIP result is also superimposed on the same figure. A linear relationship is observed over a wide range of energy depositions. A linear fit through the data points yields, $ADC = 46.7 \times E_{dep} + 26$, where E_{dep} is expressed in MeV. The offset maybe because of the electronics conversion and gain. This assures the quality of the measurement and will be useful while designing the full silicon-tungsten calorimeter.

8. Summary

In summary, we report a novel design of a sampling calorimeter using silicon pad detector arrays and tungsten converters. The performance of the calorimeter has been studied by using detailed simulation as well as by constructing a prototype mini-tower. The mini-tower consisted of four layers of silicon pad detector arrays and several tungsten plates. Two different configurations of the mini-towers have been used to probe from $1-6X_0$ depth in the longitudinal direction. Laboratory tests using ^{90}Sr source were made to ensure the good quality of the silicon pad detectors. The mini-tower was tested using pion and electron beams from 1–6 GeV. Pions give response corresponding to minimum ionizing particles, whereas electrons produce shower. The energy deposition resulting from the showers have been measured and compared with results from simulations. A linear relationship between the energy depositions in the simulation and data was obtained, which ensures

satisfactory performance of the silicon-tungsten mini-tower.

Acknowledgement

We acknowledge the support of C.K. Pithawa, Dinesh Srivastava, Yogendra Viyogi, R.K. Bhandari, Werner Riegler and Paolo Giubellino. We thank the ALICE FoCaL collaboration, especially discussions with Premomoy Ghosh, Taku Gunji, Marco Van Leeuwen, Gert-Jan Nooren, Elena Rocco and Thomas Peitzmann. We acknowledge Bharat Electronics Limited, Bangalore for providing good quality silicon detectors. We thank the CERN PS team for providing excellent quality beam for the detector tests.

References

- [1] Christian W. Fabjan and Fabiola Gianotti, *Rev. Mod. Phys.* **75** (2003) 1243.
- [2] P.G. Rancoita, *Jour. of Phys.* **G 10** (1984) 299.
- [3] P.G. Rancoita, A. Seidman, *Nucl. Instr. and Meth. in Phys. Res.* **A 263** (1988) 84.
- [4] G.Barbiellini, G.Cecchet, J.Y.Hemery, F.Lemeilleur, C.Leroy, G.Levman, P.G.Rancoita and A.Seidman, *Nucl. Instr. and Meth. in Phys. Res.* **A 235** (1985) 55.
- [5] G.Barbiellini, G.Cecchet, J.Y.Hemery, F.Lemeilleur, C.Leroy, G.Levman, P.G.Rancoita and A.Seidman, *Nucl.Instr. and Meth.in Phys. Res.* **A 236** (1985) 316.
- [6] G.Ferri, F.Groppi, F.Lemeilleur, S.Pensotti, P.G.Rancoita, A.Seidman and L.Vismara, *Nucl.Instr. and Meth.in Phys. Res.* **A 273** (1988) 123.
- [7] M. Bocciolini *et al.* (WIZARD Collaboration), *Nucl. Instr. Meth.* **A 370** (1996) 403-412.
- [8] G. Abbiendi *et al.*, (OPAL Collaboration), *Eur. Phys. J. C* **14** (2000) 373.
- [9] Jeremy Rouene *et al.* (CALICE Collaboration) *Nucl. Instr. and Meth. in Physics Research A* **732** (2013) 470.
- [10] Remi Cornat *et al.* (CALICE collaboration) *Jour. of Phys. Conference Series* **160** (2009) 012067.
- [11] E. Kistenev *et a.* (PHENIX Forward Calorimeter Collaboration) *Czechoslovak Journal of Physics*, **55** (2005) 1659.
- [12] V. Bonvicini *et al.* *IEEE Trans. Nucl. Sci.* **52** (2005) 874.
- [13] D. Strom *et al.*, *IEEE Trans. Nucl. Sci.* **52** (2005) 868.
- [14] Radha Pyari Sandhir, Sanjib Muhuri, Tapan K. Nayak, *Nucl. Inst. and Meth. in Physics Research Section A* **681** (2012) 34.
- [15] T. Peitzmann *et al.* (ALICE FoCal collaboration), arXiv:1308.2585 [physics.ins-det].
- [16] S. Agostinelli et al, *Nucl. Instr. and Meth. in Physics Research A* **506** (2013) 250.
- [17] J. Allison *et al.*, *IEEE Transactions on Nuclear Science* **53** (2006) 270-278.
- [18] P. Courtat *et al.*, "The electronics of the Alice Dimuon Tracking Chambers", ALICE Internal Note, ALICE-INT-2004-026.
- [19] ALICE Collaboration, "Addendum to the Technical Design Report of the Photon Multiplicity Detector (PMD)", ALICE TDR 6, CERN/LHCC 2003-038.
- [20] W.W.M. Allison, *Ann. Rev. Nucl. Part. Sci.*, **30** (1980) 30.